



2021년도 한국현미경학회 춘계학술대회

The Effects of Process Parameters on the Microstructure of SUS316 Fabricated by Selective Laser Melting

Sijia Liu¹, Choi Chul², and Keesam Shin^{1,*}

¹School of Materials Science and Engineering, Changwon National University, Changwon, Korea

²KEPCO Research Institute, Korea Electric Power Corporation, Daejeon, Korea

*E-mail: keesamgg@gmail.com

발표자 : Sijia Liu

Changwon National University
liusijiaa@gmail.com



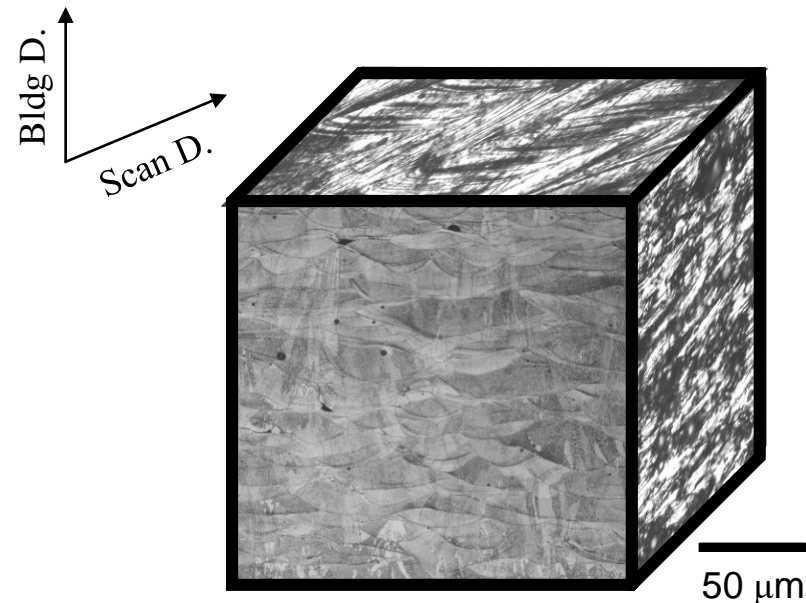
한국현미경학회
Korean Society of Microscopy

➤ Background

- ✓ The microstructure of the specimens made by additive manufacturing (AM) and laser welding is very similar, but the fatigue strength of the AM specimen is lower
- ✓ Selective laser melting (SLM) displays outstanding characteristics of full melting of the powder with highest density among the AM category. Researches show that processing parameters play a key role on the quality of the products by the SLM

➤ Objectives

- ✓ Relationship between porosity fraction and energy density
- ✓ Optimize processing parameters in this study



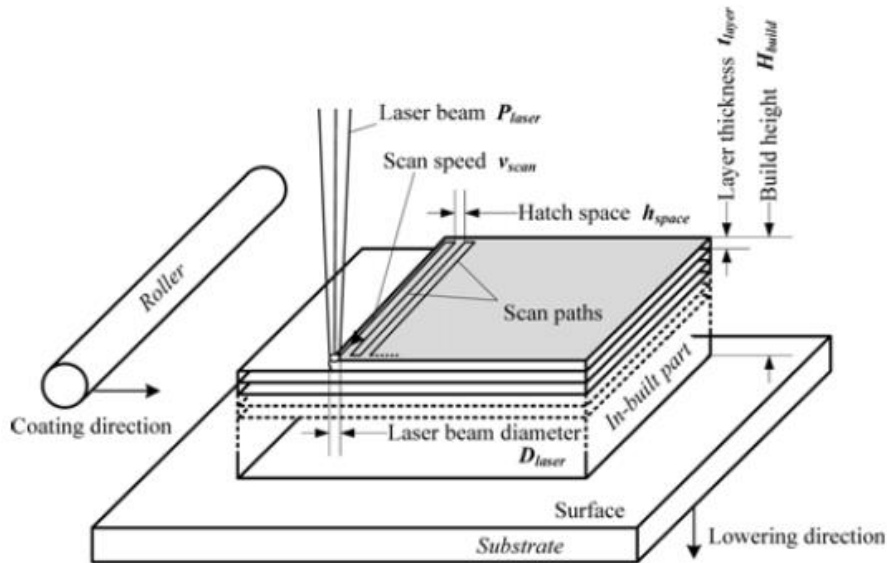
SLM280HL(SUS316L)

Table 1. Chemical composition of stainless steel 316L (reference).

Material	Fe	Cr	Ni	Mo	Mn	Si	P	S	C	N	O
316L (10~45 μm)	Bal.	16.00 ~18.00	10.00 ~14.00	2.00 ~3.00	2.00	1.00	0.045	0.030	0.030	0.10	0.04

Table 2. SLM process parameters for producing stainless steel 316L.

Laser power P (W)	Scanning speed v (mm/s)	Layer thickness t (mm)	Hatch spacing h (mm)	Laser energy density E_v (J/mm ³)
180 - 220	700 - 900	0.03	0.12	55.55 - 87.30



Energy density normally consists of four independent process parameters, (1) laser powder Plaser (W), the power value of the laser beam; (2) scan speed v_{scan} (mm/s), the velocity with which the laser beam traverses along the scan paths; (3) hatch space h_{space} (mm), the distance between two adjacent scan paths; and (4) layer thickness t_{layer} (mm), the thickness of a layer that equals the incremental amount of the lowering building bed.

Fig. 1. Schematic diagram of SLM process parameters [1].

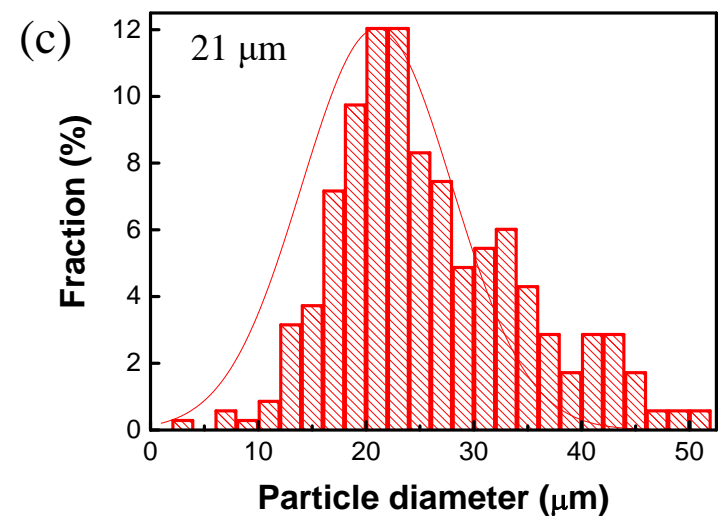
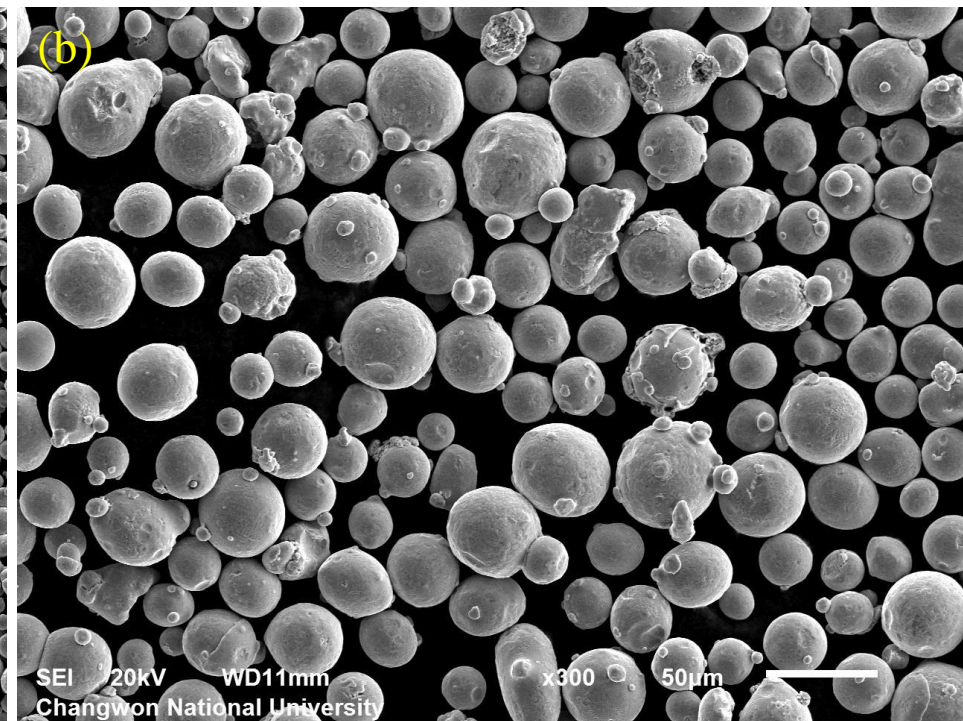
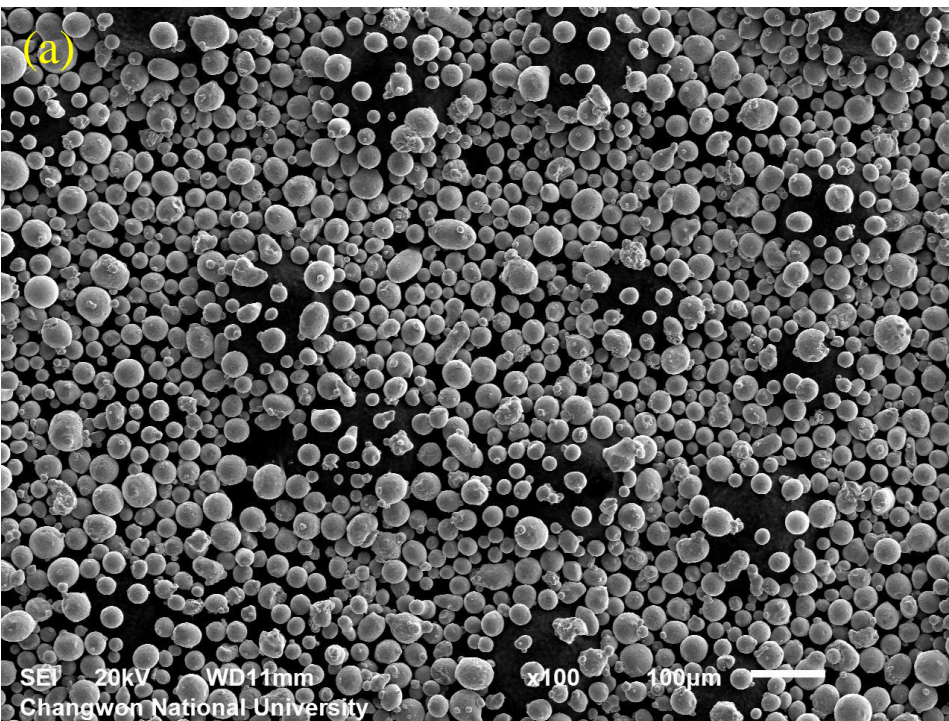


Fig. 2. SEM analysis of (a, b) SUS316L powder, and (c) particle diameter distribution.

III. Porosity measurement

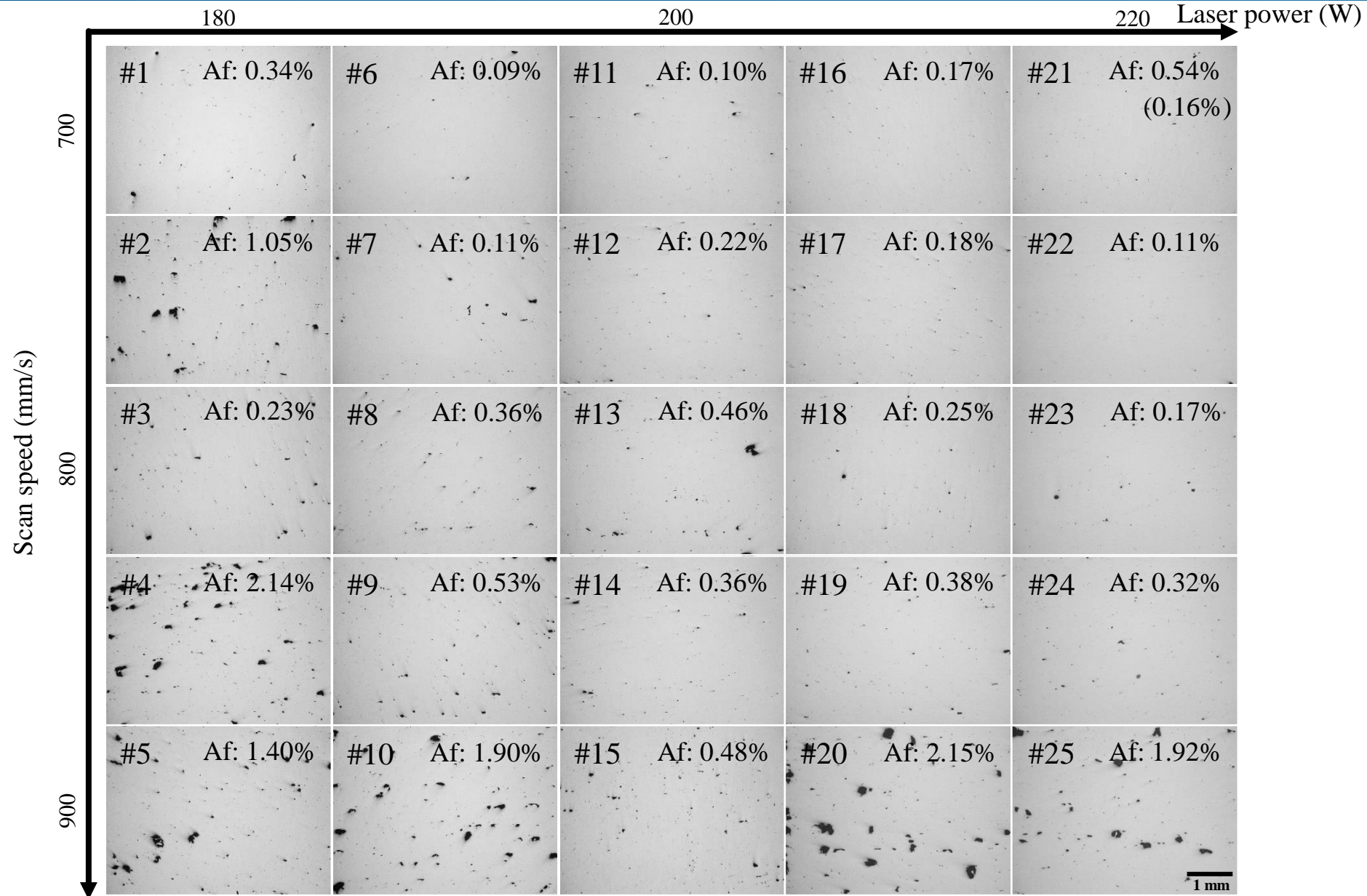


Fig. 3. The effect of changing the scan speed and laser power on porosity developed in SLM280HL.

III. Energy density-Porosity relationship

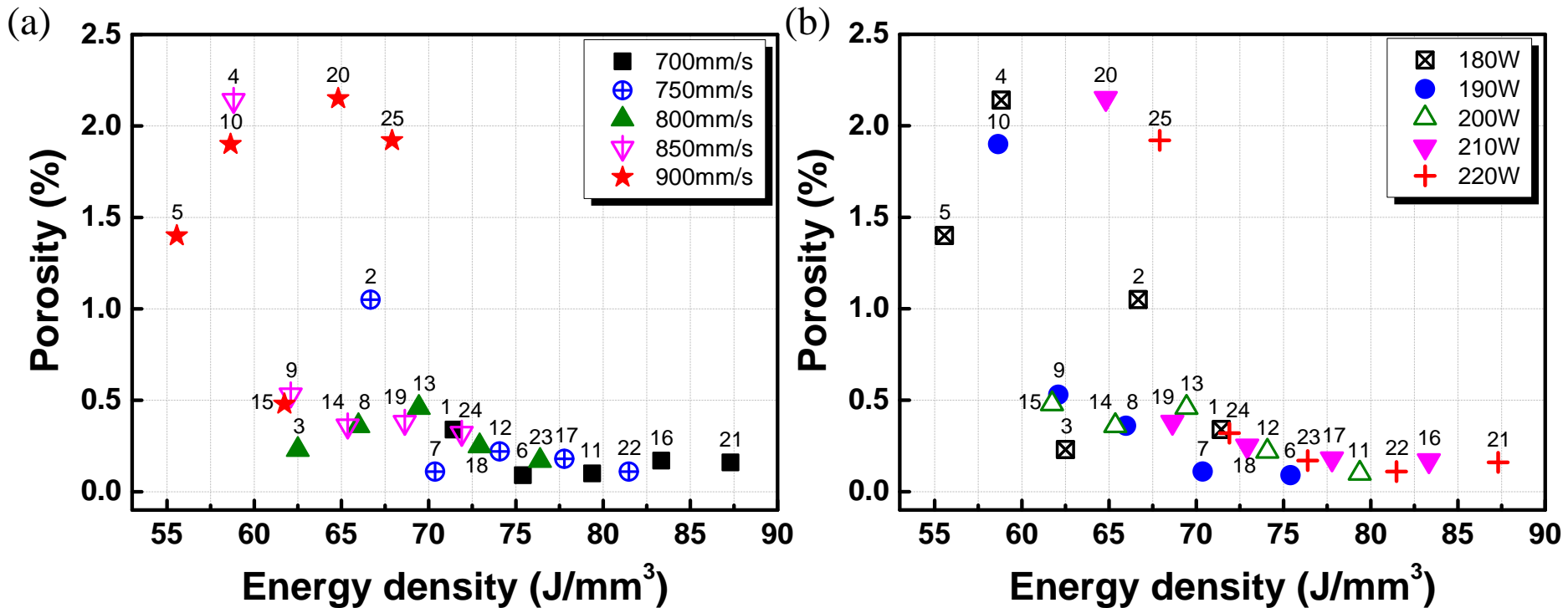
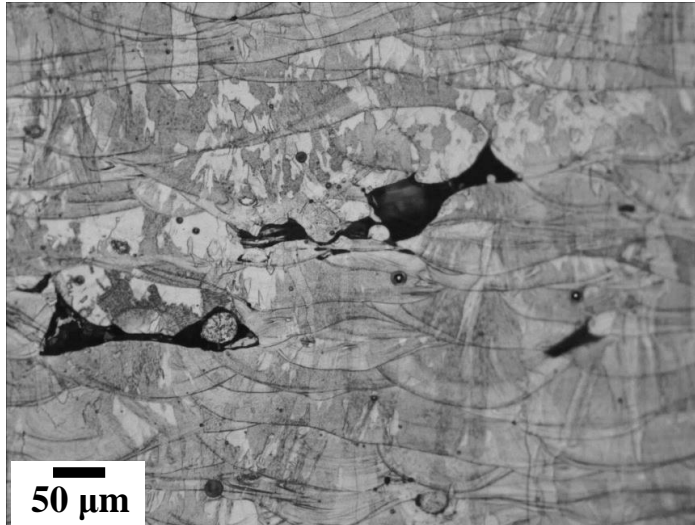


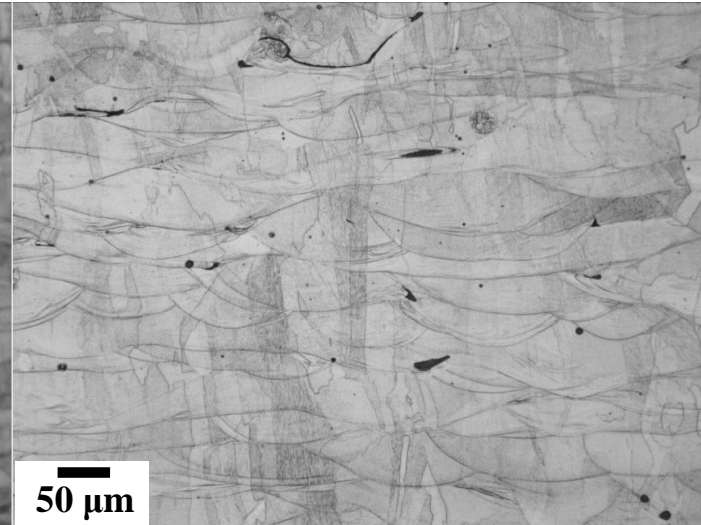
Fig. 4. The variation of porosity with energy density.

- Specimen reached a maximum of 0.5% porosity when energy density varies from **68-87 J/mm^3** , caused by slow scan speed and longer process time with higher energy consumption. When energy density varies from 55-67 J/mm^3 , the fraction of porosity reaches 0.5-2.15%.
- The quantitative analysis of microstructural defects (pores) of the specimens at various input energy densities indicated that the porosity was the lowest when fabricated at **200 W (laser power), 700 mm/s or 800 mm/s (scan speed)**.
- The fraction of porosity increased obviously at high scan speed (900 mm/s) and low laser power (180 W). In this study, lower porosity is produced at higher energy density.

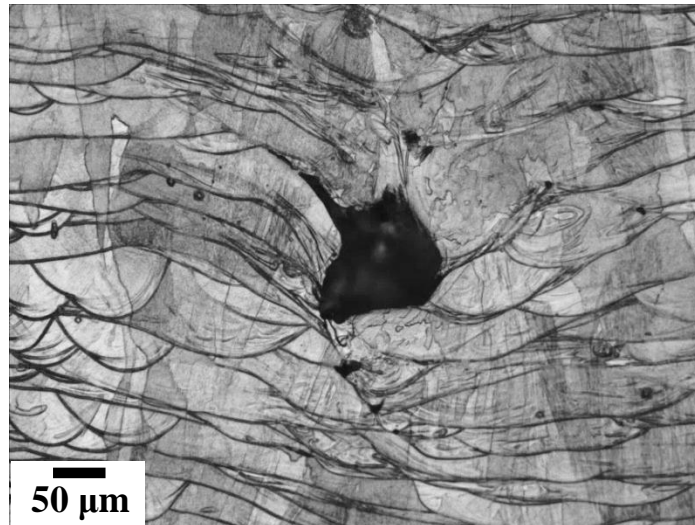
(a) #10 (190W 900mm/s)



(b) #15 (200W 900mm/s)



(c) #20 (210W 900mm/s)



(d) #25 (220W 900mm/s)

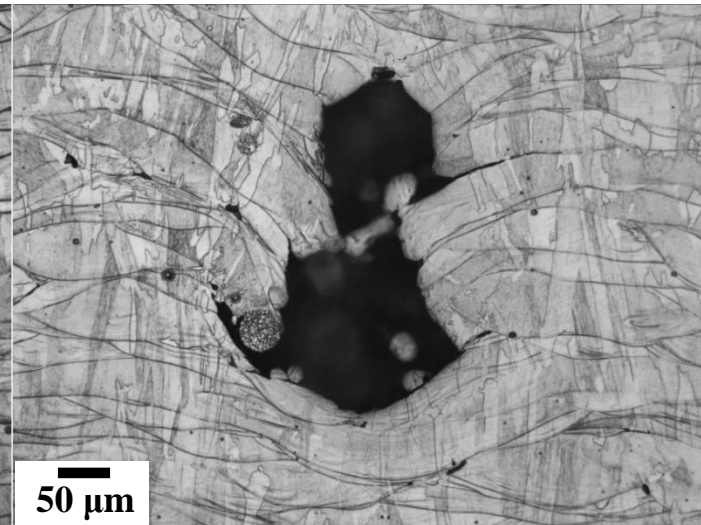


Fig. 5. Optical micrographs of the influence of the laser power on melt pool of (a) #10, (b) #15, (c) #20, and (d) #25 specimen in front view.

III. Melt pool (#13, 200W, 800mm/s)

2021
춘계학술대회



한국현미경학회
Korean Society of Microscopy

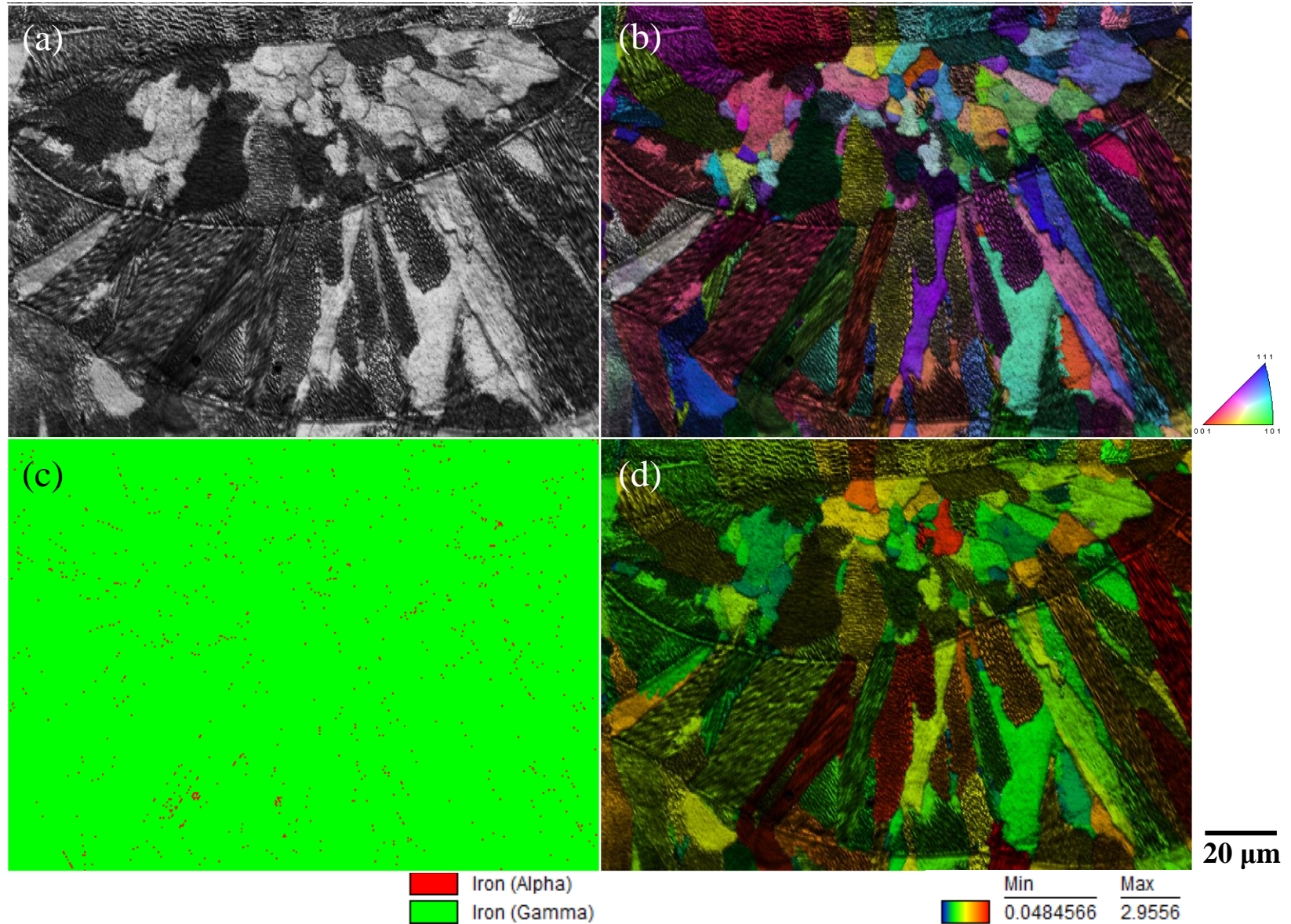


Fig. 6. EBSD analysis of (a) Image Quality, (b) Inverse Pole Figure, (c) Phase map, and (d) Grain orientation spread map of #13 specimen.

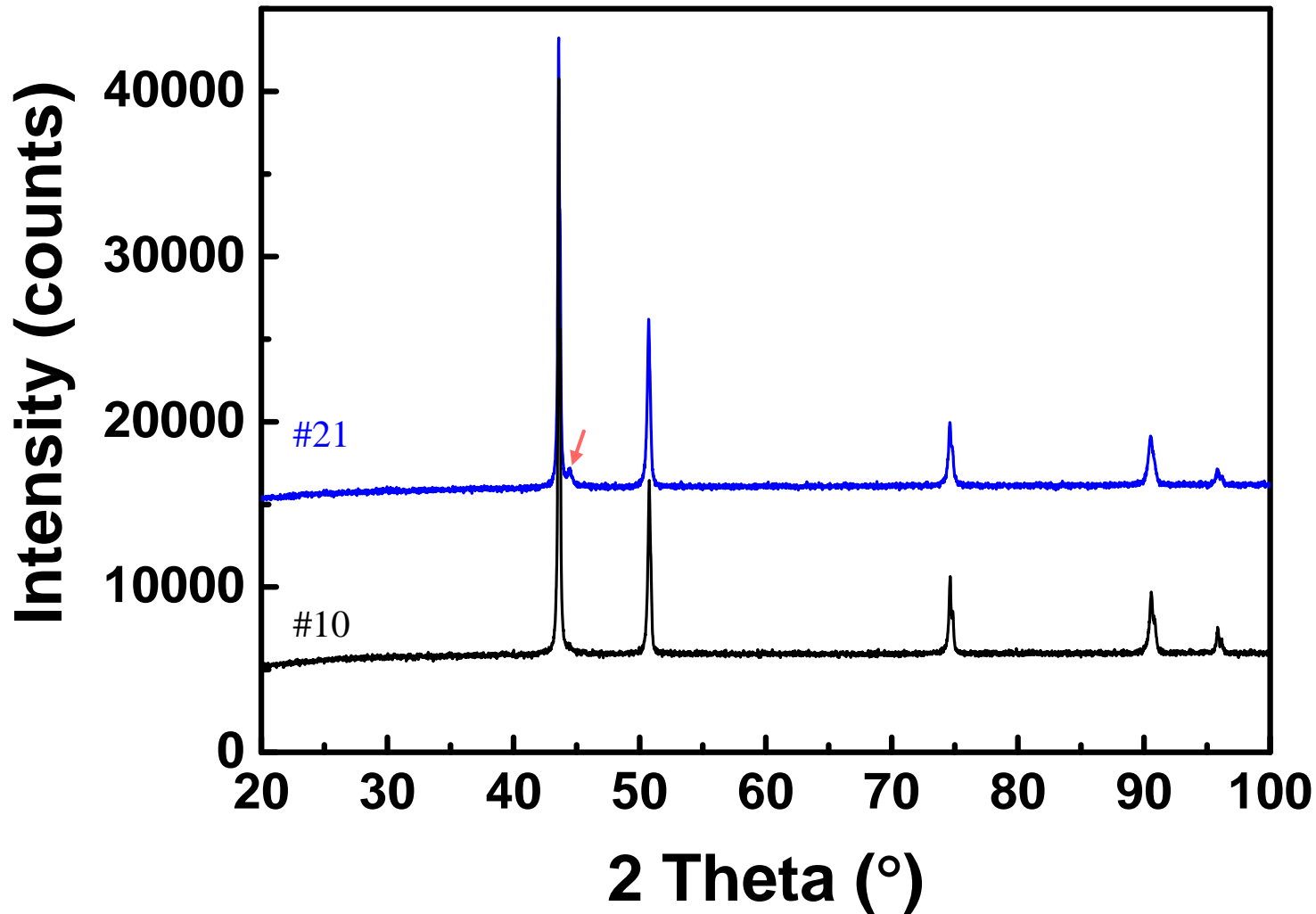


Fig. 7. XRD diffractogram of austenitic structure of #10 and #21 specimen.

- The results suggest that **input energy density must be maintained at $\sim 70 \text{ J/mm}^3$ or higher for porosity fraction of 0.5% or lower**, in which scan speed did not affect the porosity fraction. At energy densities lower than 68 J/mm^3 , a higher scan speed results in higher porosity.
- **Fluctuation of porosity fraction** (up to 1.55%) exist at similar energy density, thus microstructural effect of melt pool is taken into consideration.
- **Keyhole pores** are the main reason for the high porosity fraction.
- Melt pools with narrow width and shallow depth resulted in **insufficient overlap** during melting, unmelted powder existing as a nucleation point, and irregular melt pool boundaries accelerating crack propagation. Herein, **spherical gas-induced pores** were observed in the melt pool.

2021 한국현미경학회 춘계학술대회



한국현미경학회
Korean Society of Microscopy